Ceramics-Silikáty 63 (4), 374-379 (2019)
www.ceramics-silikaty.cz doi: 10.13168/cs.2019.0033

EFFECTS OF AGGREGATE CONTENT ON THE INTERCONNECTED PORE FORMATION AND PROPERTIES OF POROUS PURGING PLUG MATERIALS

#QINGHENG WANG*, **, ANPING DONG*, WENDONG QIU**, YUANBING LI***, GUOZHI RUAN**, LANQIN ZHANG**

*School of Materials Science and Engineering, Shanghai Jiao Tong University, Shanghai 200240, China
**Shanghai Baosteel Industry Technological Service Co.Ltd., Shanghai 201900, China
***The State Key Laboratory of Refractories and Metallurgy, Wuhan University of Science and Technology (WUST), Wuhan 430081, China

#E-mail: wqhref@163.com

Submitted April 9, 2019; accepted August 5, 2019

Keywords: Firing temperature, α-Aluminum hydroxide, Microstructure

The physical properties and microstructure of porous purging plug materials with different aggregate contents and prepared at different firing temperatures were investigated by means of X-ray diffraction, scanning electron microscopy, air permeability, pore size distribution, apparent porosity, bulk density, cold modulus of rupture (CMOR), cold elastic modulus (E) and cold crushing strength (CCS) tests. The results show that the aggregate content had a great effect on the interconnected pore formation and properties of porous purging plug materials. With decreasing aggregate content, the apparent porosity and air permeability increased due to the distance between aggregates increasing and $Al(OH)_3$ formation, and the pore size distributions changed from a monomodal distribution to a bimodal distribution. The higher temperature facilitated the formation of a denser structure and interconnected pores. In addition, the CCS and porosity were found to follow a simple exponential relationship. When the apparent porosity increased, the CCS decreased, and vice versa.

INTRODUCTION

Secondary refining technology was introduced to produce high-quality and pure steel, as the purging plug installed at the bottom of the ladle is being used extensively to homogenize the temperature and composition of molten steel by stirring with argon and to promote the flotation of non-metallic inclusions. Hence, the purging plug is the most pivotal functional part of this process. Mainly, three types of purging plugs have been commonly used over the past few decades, including porous-type, directional-type and slit-type plugs [1]. Compared to the directional-type and slit-type plugs, the porous-type plug has a better bubbling reliability [2] and a better capability to remove impurities from the molten steel. Interconnected pores are the key structural feature of it. Hence, the preparation of interconnected pores is of great significance in steel-making applications.

The interconnected pore structure can be formed through the techniques mentioned below, including direct foaming [3-6], replica templating [7], adding pore-forming agents [8-10] and so on, but the pore size by direct foaming and the replica template method is much bigger than what would be suitable to be used in steel-making applications. The method of incorporation of pore-forming agents with ceramic powder results can yield a porous structure of closed or poorly interconnected pores. Considerable research work directed at interconnected pore formation has been performed in our group [11-14]. The formation of interconnected pores is affected not only by the aggregate size [11] and content, but also by the pore-forming agent size [12] and content. Larger aggregates facilitated pore linkage, which is beneficial to the formation of interconnected pores [11]. Point contact between aggregates is favorable for the formation and connectivity of the pores (Figure 1). A smaller particle size of $Al(OH)_3$ was suitable to induce the formation of interconnected pores [12] and a higher $Al(OH)_3$ content is beneficial to the pore formation after high-temperature treatment.

It is well known that the aggregate is difficult to sinter. Higher aggregate content will reduce the physical properties of the materials and lower aggregate content will affect the interconnected pores formation. Hence, in this paper, the effect of aggregate content on the interconnected pore formation and properties of porous purging plug materials was investigated by introducing $Al(OH)_3$ to increase the number of pores in the materials.

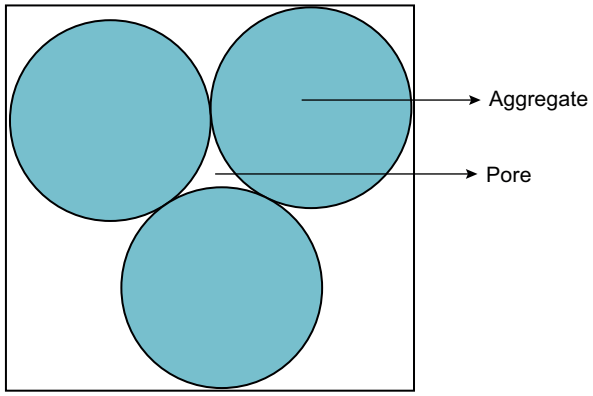

Figure 1. Schematic illustration of the particle packing model.

EXPERIMENTAL

Specimen preparation

Tabular alumina (0.5 - 1 mm, 98 wt. % Al_2O_3, Zhejiang Zilialumina Material Technology Co., Ltd. China), $Al(OH)_3$ (Chalco Shandong Advanced Material Co., Ltd. China), microsilica powder (951UL, Elkem, Norway) and $CaCO_3$ (≥ 99.0 %, Sinopharm Chemical Reagent Co., Ltd.) were used as the main raw materials. The detailed compositions are provided in Table 1. The microsilica and $CaCO_3$ in these compositions were used as sintering agents. In order to distribute the materials evenly, the main raw materials were first blended in a rotor drum for 3 h at a rotation rate of 30 rotations per min. Additionally, a 2.5 wt. % PVA solution (2 wt. % concentration) was used as binder. Cylindrical specimens (50 mm × 50 mm) and rectangular specimens (140 mm × × 25 mm 5 × 25 mm) were prepared by uniaxial die pressing at 100 MPa. All specimens were dried at 110 °C for 24 h. Finally, the specimens were fired at 1600 °C and 1650 °C, with a heating rate of 3 °C per min and a holding time of 3 h before cooling to room temperature.

Test and characterization methods

Apparent porosity and bulk density were characterized via the Archimedes method, using water as the immersion liquid. Air permeability values were obtained according to the Chinese standard GB/T 3000-1999. Pore size distribution and pore size intervals were measured using mercury intrusion porosimetry (Quantachrome PM60GT-18, Quantachrome Instruments Ltd., USA). The modulus of elasticity (E) was determined by the impulse excitation measurements (RFDA professional, IMCE, Belgium) at room temperature. The cold modulus of rupture (CMOR) was measured by three-point bending at room temperature. The cold crushing strength (CCS) was evaluated using a hydraulic testing machine. The microstructure of the specimens was analyzed by scanning electron microscopy (SEM, JSM-6610, JEOL, Japan).

Table 1. Detailed composition of specimens.

Raw materials	wt. %					
	A	B	C	D	E	F
Tabular alumina (0.5 - 1 mm)	80	75	70	65	60	55
$Al(OH)_3$ (0.088 mm)	15	20	25	30	35	40
SiO_2 powder (0.5 μm)	2	2	2	2	2	2
$CaCO_3$ (–)	3	3	3	3	3	3

RESULTS AND DISCUSSION

Figure 2 shows the apparent porosity and bulk density with different content of aggregate. The apparent porosity increased with decreasing aggregate content, and is higher for specimens fired at 1600 °C than for specimens fired at 1650 °C. The bulk density exhibited exactly the opposite trends. The increase in apparent porosity and the corresponding decrease in bulk density was attributed to the introduction of $Al(OH)_3$. The $Al(OH)_3$ in the specimens can form a large amount of pores [12] after thermal treatment. Higher temperature facilitated the sintering process and made the structure

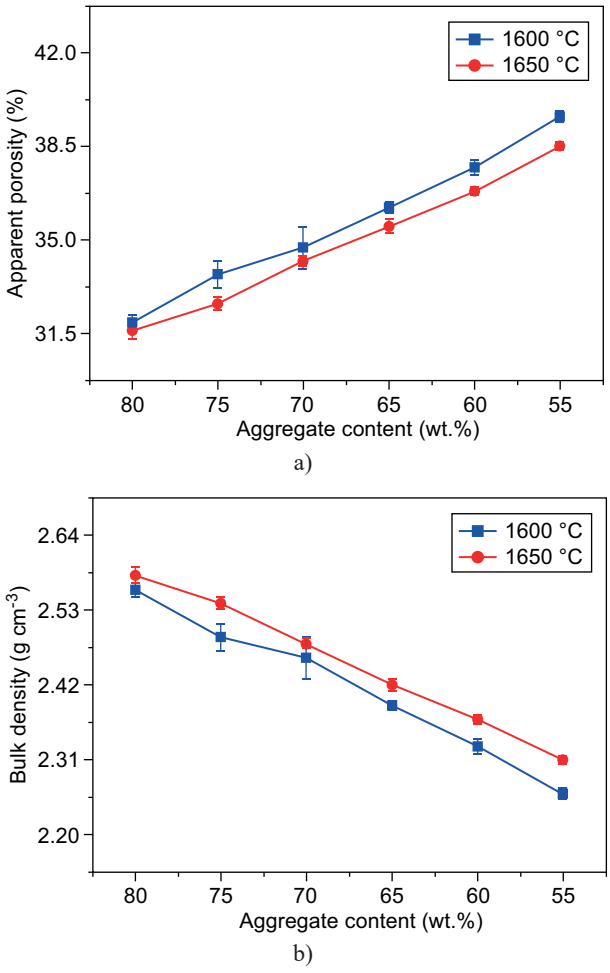

Figure 2. Apparent porosity and bulk density of specimens with different aggregate content.

of specimens denser, which resulted in a decrease of apparent porosity and a corresponding increase of bulk density.

The air permeability of specimens with different content of aggregate is shown in Figure 3. With decreasing aggregate content, the air permeability increased, i.e. the latter exhibits the same trend as the apparent porosity. However, with an increase of the firing temperature from 1600 °C to 1650 °C, all specimens showed increased air permeability, which is a result that is opposite to the apparent porosity. These unexpected and surprising results may be due to the following reasons. When the aggregate content is higher, the distance between aggregates is small, and the amount of $Al(OH)_3$ filling the gaps between the aggregates is small. After thermal treatment, the amount of pores between aggregates is small and the apparent porosity and air permeability is small. With the increase of aggregate content, the distance between aggregates become larger, and the amount of $Al(OH)_3$ filled in the gap between the aggregates become more. After thermal treatment, the apparent porosity and air permeability have the same tendency to change, that is, gradually increase. In addition, the shrinkage difference between aggregates and matrix can also form pores [12] and may contribute to the pore connectivity. With the increase of temperature, the shrinkage difference is even more pronounced, resulting in an increase in the number of interconnected pores, which is beneficial to the improvement of air permeability; moreover, with the

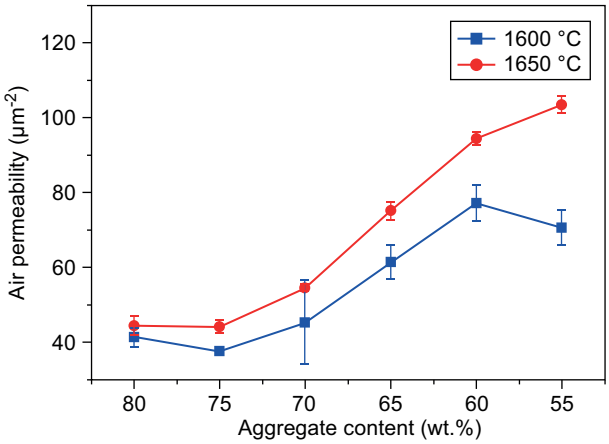

Figure 3. Air permeability of specimens with different aggregate content.

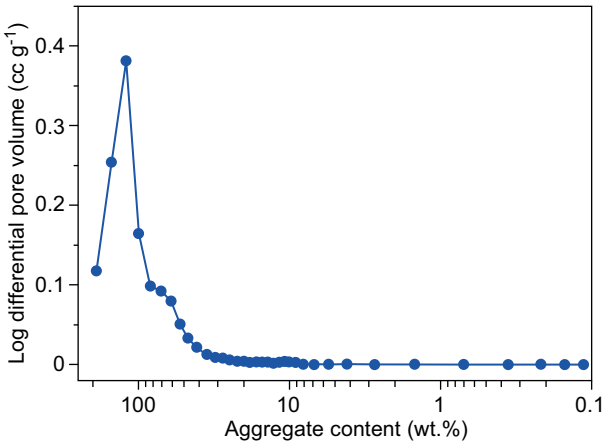

a)

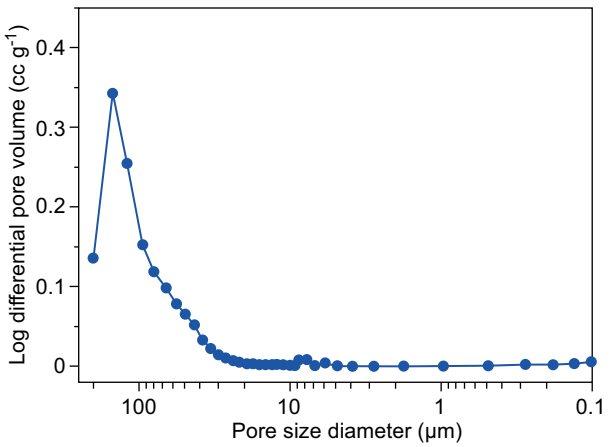

b)

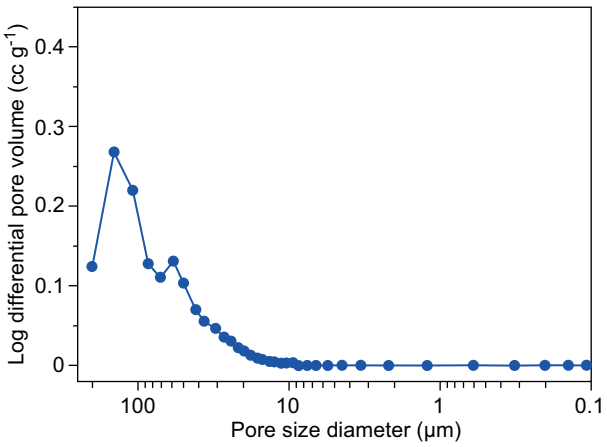

c)

Figure 4. Pore size distribution of specimens with different aggregate content.

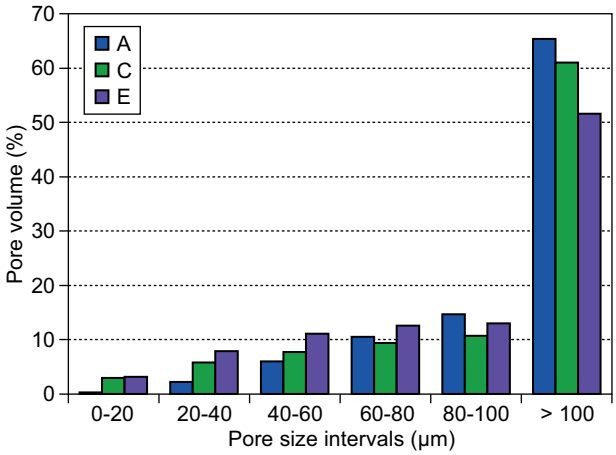

Figure 5. Pore volume of different intervals of specimens with different aggregate content.

increase of temperature, the structure becomes denser and the number of pores decreases, leading to a decrease of apparent porosity.

Figure 4 shows the pore size distribution of specimens with different aggregate content after firing at 1600 °C. When the aggregate content is higher, the pore size distributions presented a unimodal distribution, while with the decrease of aggregate content, the pore size distributions becomes more bimodal. Figure 5 presents the pore volume of different intervals of specimens with different aggregate content.

The effect of aggregate content on the CMOR and E of specimens after firing at 1600 °C is shown in Figure 6. It can be seen that the CMOR and E have the same trends. The CMOR and E decreased nonlinearly. Figure 7 shows the effects of aggregate content on the CCS of the specimens after firing at 1600 °C. It can be seen that also the CCS of the specimens tended to decrease nonlinearly, in contrast to the apparent porosity (Figure 2), which increases more or less linearly. Rice advocated the use of a simple exponential relationship used to describe the dependence of strength (σ) on (total) porosity (P) [15]. This relation is:

$$\sigma = \sigma_0 \exp(-bP),$$

where σ_0 is the strength of the specimens without pores, and b is a constant associated with the pore characteristics. From this relation, it can be seen that strength decreased with increasing porosity. The results obtained in this work were found to follow this relationship with a b value of … (obtained by fitting). As the apparent porosity increased, the CCS decreased.

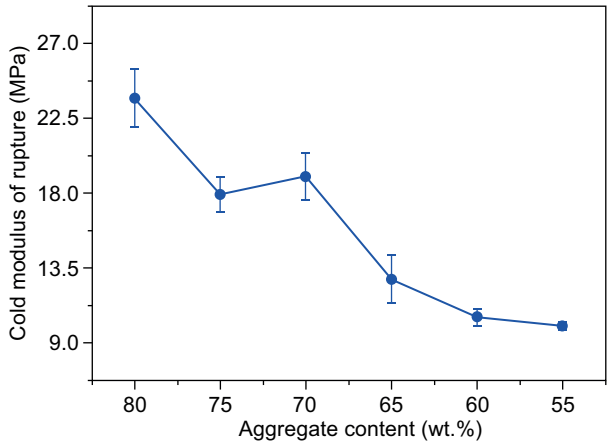

a)

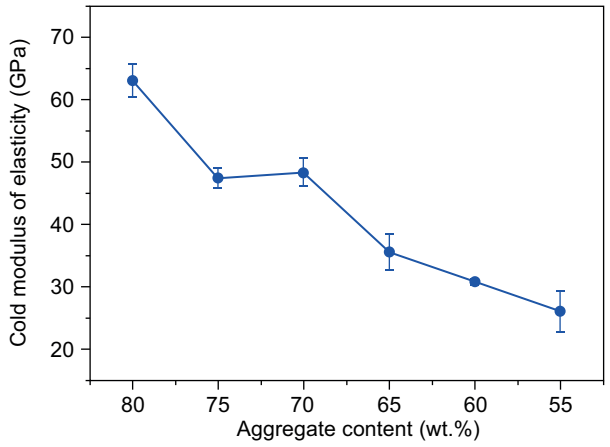

b)

Figure 6. CMOR and E of specimens with different aggregate content.

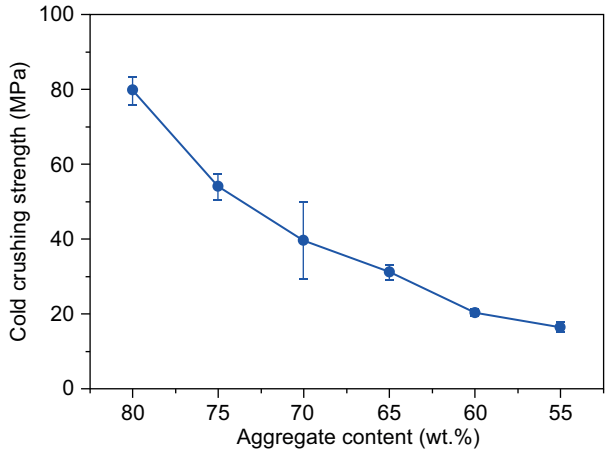

Figure 7. CCS of specimens with different aggregate content.

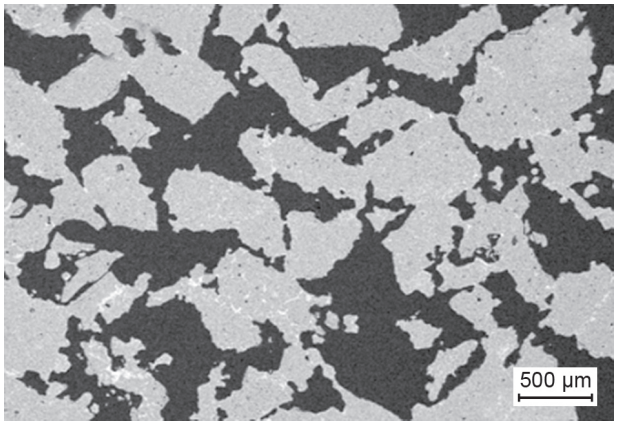

a)

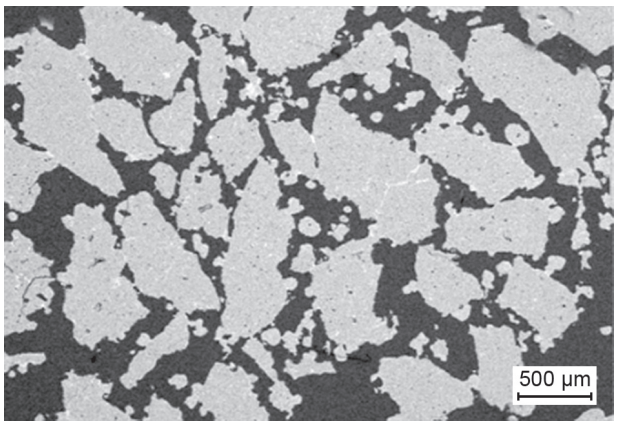

b)

Figure 8. Microstructure of specimens with different aggregate content after firing at 1600 °C. *(Continue on next page)*

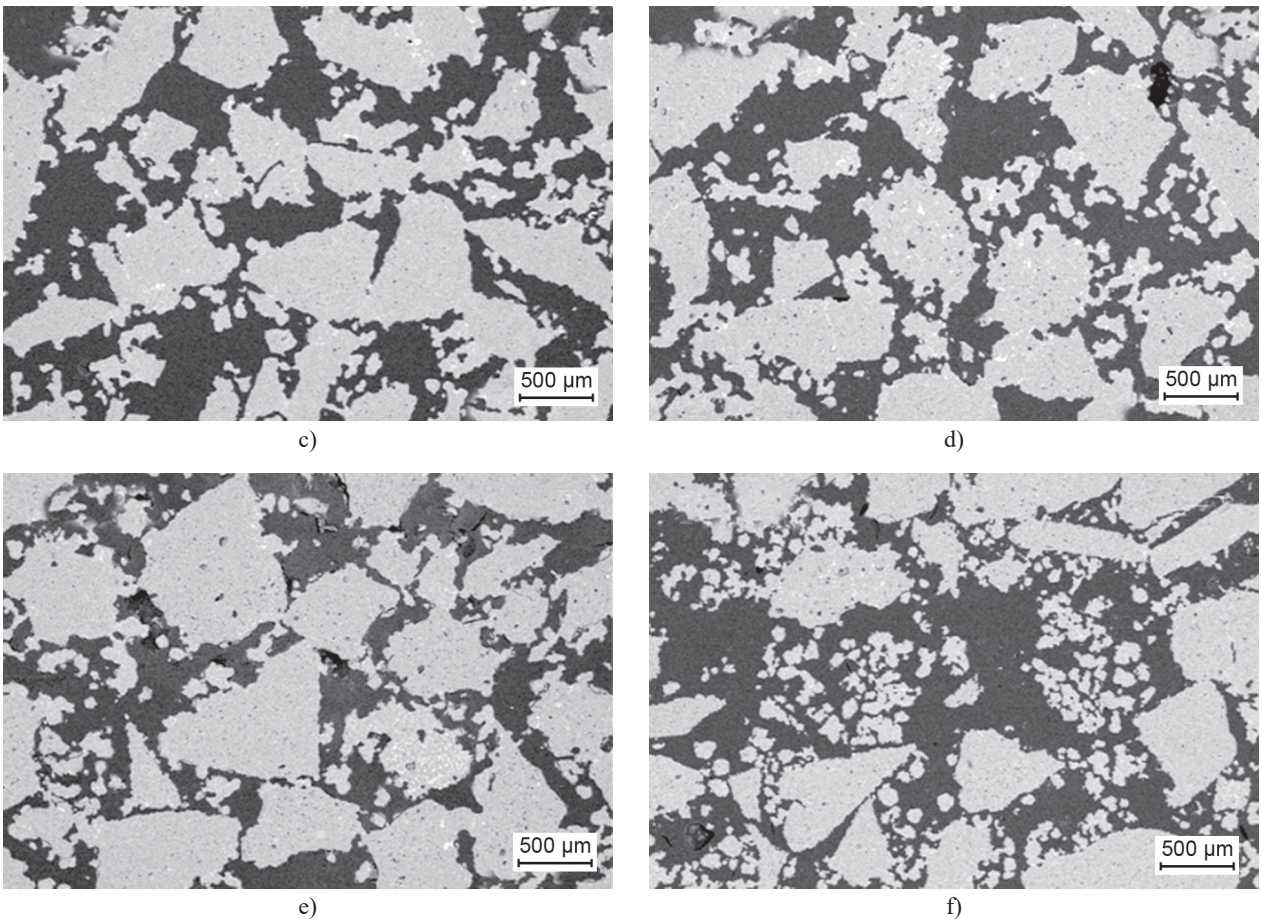

c) d) e) f)

Figure 8. Microstructure of specimens with different aggregate content after firing at 1600 °C.

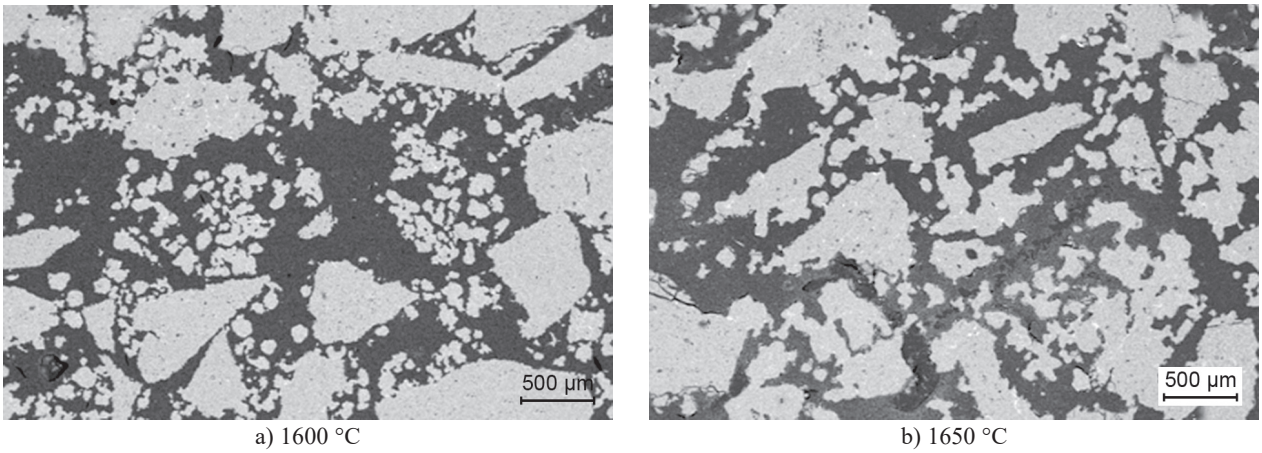

a) 1600 °C b) 1650 °C

Figure 9. Microstructure of specimen F after firing at 1600 °C and1650 °C.

Figure 8 shows the microstructure of specimens A, B, C, D, E, F after firing at 1600 °C. When the aggregate content is 80 wt. %, the distance between aggregates is small, and less pores were formed. When the aggregate content is 55 wt. %, the distance between aggregates is large, and a large amount of $Al(OH)_3$ filled the gap between the aggregates. After thermal treatment, a large amount of pores can be formed. Hence, with the decrease of aggregate content, the structure became more and more loose and the amount and size of pores increased. Figure 9 shows the microstructure of specimens F after firing at 1600 °C and 1650 °C. When the sintering temperature was 1600 °C, some big pores and independent pores existed in the structure. After sintering at higher temperature (1650 °C), the pores show a high level of interconnectivity, which is beneficial to the improvement of air permeability.

CONCLUSION

The aggregate content had a significant effect on the interconnected pore formation and properties of porous purging plug materials. With decreasing aggregate content, the apparent porosity and air permeability increased, because the distance between the aggregates increased and introduction of $Al(OH)_3$ as well as the pore size distributions changed a unimodal distribution to a bimodal distribution. The higher firing temperature facilitated the formation of a denser structure and highly interconnected pores. In addition, the porosity dependence of the CCS was found to follow the relationship $\sigma = \sigma_0 \exp(-b\,P)$ with $b = \ldots$. When the apparent porosity increased, the CCS decreased, while when the apparent porosity decreased, the CCS increased.

REFERENCES

1. Xue W. (2003). Study on composition and slit design and application of purging plug used in steel ladle. University of Science and Technology Beijing, pp. 10-12 (In Chinese).
2. Kimura M., Ohuchi T., Tsuzuki T., et al. (2001). Development and application of porous type gas purging plug with high bubbling reliability and durability. In: Proceedings of UNITECR'01, Cancun, Mexico.
3. He X., Su, B. Tang Z., Zhao B., Wang X., Yang G., et al (2012): The comparison of macroporous ceramics fabricated through the protein direct foaming and sponge replica methods. Journal of Porous Materials. 19, 761-766. doi: 10.1007/s10934-011-9528-z
4. Li F., Kang Z., Huang X., Wang X. G., Zhang G. J. (2014): Preparation of zirconium carbide foam by direct foaming method. Journal of the European Ceramic Society, 34, 3513-3520. doi: 10.1016/j.jeurceramsoc.2014.05.029
5. Li Y., Cao W., Feng J., Gong L., Cheng X. (2015): Fabrication of cordierite foam ceramics using direct foaming and slip casting method with plaster moulds. Advances in Applied Ceramics, 114, 465-470. doi: 10.1179/1743676115Y.0000000022
6. Xu C., Wang S., Flodström K., Mao X., Guo J. (2010): Cellular silica-based ceramics prepared by direct foaming at high temperature. Ceramics International, 36, 923-927. doi: 10.1016/j.ceramint.2009.10.023
7. Studart A. R., Gonzenbach U. T., Tervoort E., Gauckler L. J. (2006): Processing routes to macroporous ceramics: a review. Journal of the American Ceramic Society, 89, 1771-1789. doi:10.1111/j.1551-2916.2006.01044.x
8. Liu J., Li Y., Li Y., Sang S., Li S. (2016): Effects of pore structure on thermal conductivity and strength of alumina porous ceramics using carbon black as pore-forming agent. Ceramics International, 42, 8221-8228. doi: 10.1016/j.ceramint.2016.02.032
9. Xu N. N., Li S. J., Li Y. B., Yuan L., Zhang J. L., Wang L., et al (2014): Fabrication and characterisation of porous mullite ceramics from high voltage insulator waste. Advances in Applied Ceramics, 114, 93-98. doi:10.1179/1743676114y.0000000195
10. Li S., Li N., Li Y. (2008): Processing and microstructure characterization of porous corundum-spinel ceramics prepared by in situ decomposition pore-forming technique. Ceramics International, 34, 1241-1246. doi: 10.1016/j.ceramint.2007.03.018
11. Wang Q.H., Li Y.B., Li S.J., et al (2017): Effects of critical particle size on properties and microstructure of porous purging materials, Materials Letters, 197, 48-51. doi: 10.1016/j.matlet.2017.03.129
12. Wang Q.H., Li Y.B., Li S.J., et al (2017): Effects of particle size of $Al(OH)_3$ on the properties of porous purging materials. Journal of the Ceramic Society of Japan, 125, 504-508. doi: 10.2109/jcersj2.16223
13. Wang Q., Li Y., Li S., et al (2017): Effects of nano-alumina content on the formation of interconnected pores in porous purging plug materials. Ceramics International, 43, 16722-16726. doi: 10.1016/j.ceramint.2017.09.064
14. Wang Q , Li Y , Xu N, et al (2018): Microstructure and phase evolution of cement-bonded high alumina refractory castables for porous purging plug. Journal of Ceramic Science and Technology, 9, 1-6. doi: 10.4416/JCST2017-00044
15. Rice R. W. (1993): Comparison of stress concentration vs. minimum solid area based mechanical property-porosity relations. Journal of Materials Science, 28, 2187-2190. doi:10.1007/BF00367582.